LOW LOSS MICROMACHINED LEAD ZIRCONATE TITANATE, CONTOUR MODE RESONATOR WITH 50Ω TERMINATION

S.S. Bedair[1], J.S. Pulskamp[1], R.G. Polcawich[1], D. Judy[1], A. Gillon[1], S. Bhave[2] and B. Morgan[1]
[1]U.S. Army Research Laboratory, Adelphi, Maryland 20783, USA
[2]OxideMEMS Laboratory, Cornell University, Ithaca, New York 14853, USA

ABSTRACT

This paper reports lead zirconate titatanate (PZT)-on-silicon electromechanical resonators with excellent, 50 Ω terminated, performances for RF applications. A low 2.14 dB insertion loss is demonstrated for a length extensional, PZT-on-2-µm-silicon 15 MHz resonator. A 22 dB return loss and maximum unloaded quality factor, $Q_{UL,max}$, of ~540 in air resulted for this resonator. Similar performances with a $Q_{UL,max}$ of 2850 are also demonstrated with a PZT fabricated on 10-µm-silicon device. The competing effects of decreased motional resistance and increased transducer capacitances with increased transduction area are addressed through analytical models and experimental results. Additionally, a third order length extensional mode piezoelectric resonator with asymmetric input and output electrodes were also designed to assess its potential performance as a piezoelectric resonant transformer; a 2.1x voltage boost is demonstrated for a 14.7 MHz extensional mode resonator.

INTRODUCTION

Prior RF-MEMS resonator research has shown promising device performances for RF systems over a wide frequency range [1-7]. Their potential use as timing references and narrow band RF filters show considerable promise while preserving the contour-mode specific advantages of MEMS, i.e. single-chip, multi-frequency integration. In addition, integrated resonant piezoelectric transformers have been explored as impedance transformers for impedance matching in RF applications [8] as well as voltage and power transformers in alternate applications such as high frequency switched mode power supplies [9] [10].

Resonators with low motional resistances are motivated by the desire for low loss and high efficiency devices. Thin film piezoelectric materials such as PZT and aluminum nitride have demonstrated low motional resistances due to the transducers' high electromechanical coupling. PZT is an attractive choice for RF MEMS resonators and resonant transformers due to its large electromechanical coupling factors and stress constants. The high field PZT non-linearity also allows for electric field tuning of the dielectric, elastic, piezoelectric constants and coupling factors; enabling resonant frequency tuning which is an attractive feature for RF systems.

In the current article, we report on higher order extensional mode PZT on silicon resonators with excellent performance. Low insertion losses (~2.1 dB) and high return losses (~22 dB) are reported. These are the lowest insertion and highest return losses with 50 Ω termination reported for thin-film PZT resonators and, to the authors' best knowledge, for thin-film contour mode piezoelectric resonators. Analytically modeled insertion loss trends, confirmed with experimental results, show the competing effects of reduced motional resistance, R_m, and increased transducer capacitances when considering increased piezoelectric transduction area. The potential utility of these resonators as piezoelectric transformers are also assessed through a brief analysis and initial experimental results.

RESONATOR DESIGN & THEORY

Figure 1 illustrates the contour-mode, PZT-on-silicon two-port devices under consideration. The motional resistances were derived first by describing the modal force based on the electrode pattern to define the induced modal stress profile. The constitutive equations of piezoelectricity were then used to relate induced stress to piezoelectric current and the resulting motional resistances were determined. This differs slightly from previously derived motional resistances [3, 4] due to differences in the modal force description [11]. The motional resistances derived for the fundamental ($R_{m,1}$) and high order ($R_{m,n}$) extensional modes, where the mode number, n, is odd, are

$$R_{m,1} = \frac{\pi^2 w_{tot} t_{tot} \sqrt{Y_c \rho_c}}{16 w_{elec}^2 Q e_{31}^2}, \qquad R_{m,n} = \frac{n}{n^2-1} \frac{\pi^2 w_{tot} t_{tot} \sqrt{Y_c \rho_c}}{4 w_{elec}^2 Q e_{31}^2} \quad \text{(1a), (1b)}$$

where e_{31} is the effective piezoelectric stress constant, Q is the quality factor, t_{tot} the total device thickness, Y_c the composite modulus, ρ_c the composite density, w_{tot} the

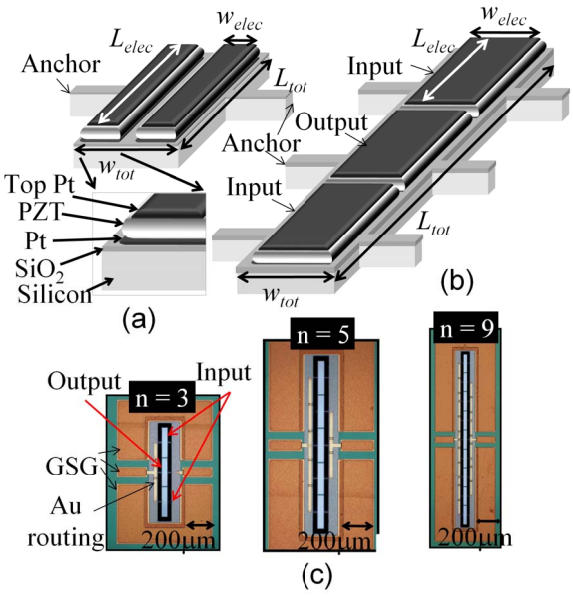

Figure 1: Illustrations of the devices under consideration: (a) fundamental length extensional mode, n = 1, with w_{elec} = 14µm and (b) example higher order length extensional mode (n = 3). (c) Top view of example fabricated devices (n = 3, 5, and 9).

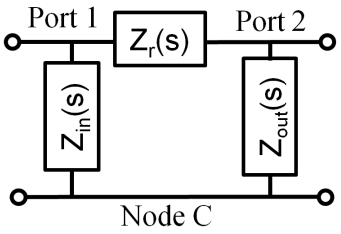

Figure 2: Two port equivalent circuit of the resonator illustrating the relevant impedances.

device width, and w_{elec} is the electrode width.

Figure 2 represents the equivalent circuit model of the two port resonator device where $Z_r(s)$ is the resonator motional impedance, $Z_{in}(s)$ the impedance of the transducer's input capacitance at port 1, $Z_{out}(s)$ the impedance of the output capacitance at port 2 and s is the complex variable equivalent to $j\omega$, where ω is the frequency. The transmission ($ABCD$) matrix is derived for this two port network

$$ABCD = \begin{bmatrix} 1+\frac{Z_r(s)}{Z_{out}(s)} & Z_r(s) \\ \frac{1}{Z_{out}(s)}+\frac{1}{Z_{in}(s)}+\frac{Z_r(s)}{Z_{in}(s)Z_{out}(s)} & 1+\frac{Z_r(s)}{Z_{in}(s)} \end{bmatrix} \quad (2)$$

and the frequency dependent scattering parameters are subsequently realized via a two-port network conversion (lookup table in [12]). The forward transmission coefficient, S_{21}, of the two port device (Figure 2) is

$$S_{21} = \frac{2}{2+\left(Z_r(s)+Z_o\right)\left(\frac{1}{Z_{out}(s)}+\frac{1}{Z_{in}(s)}\right)+\frac{Z_r(s)}{Z_o}+\frac{Z_oZ_r(s)}{Z_{in}(s)Z_{out}(s)}} \quad (3)$$

where Z_o is the characteristic impedance (50 Ω). It is evident from Equations (1a) and (1b) that minimizing the motional resistance is attained by either increasing the transducer width or using a higher order harmonic. This, however, trades with increased capacitances at the input and output ports. Increased capacitances result in lower impedances and larger shunt currents to the common node (Node C) in Figure 2. These competing effects are especially important since PZT has a relatively high dielectric constant, ε_r (400-1000), when compared with aluminum nitride ($\varepsilon_r \sim 10$), therefore, changes in the PZT transducer area have a larger effect on the transducer capacitances.

Figure 3 shows the insertion loss trend with larger n evaluated at the device resonant frequency. PZT is compared to a device with typical aluminum nitride (AlN) properties. Note that the comparison is made with 0.5 µm of piezoelectric material on 10 µm of device silicon for geometries and resonant frequencies addressed in this paper: w_{tot} = 40 µm, L_{elec} = 196 µm, and w_{elec} = 36 µm (w_{elec} is 14 µm for n = 1). However, a similar analysis can be made with varying device geometries at a variety of resonant frequencies. Typical PZT properties (effective piezoelectric stress constant, e_{31} = 12, and dielectric constant, ε_r = 400) are used with varying Q's, as indicated in the figure [13]. The trends show an optimal n (or device area) for a given quality factor. Increasing n has

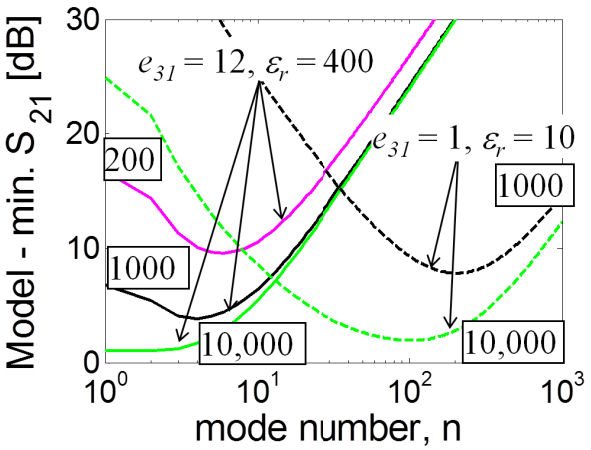

Figure 3: Trend for minimum insertion loss for 0.5µm PZT on 10µm Si, ~20MHz resonator. This is based on a two port circuit model in Figure 2 assuming operation at the device's resonant frequency. The typical properties of PZT (e_{31} = 12, ε_r = 400) are used to compare these trends with varying quality factors which are indicated. As a comparison, the expected trend for a 0.5 µm AlN device on 10 µm silicon is included (e_{31} = 1, ε_r = 10).

faster diminishing returns for PZT devices as compared with AlN type devices. With a similar Q, the optimal area, yielding the best performance of AlN type devices occurs at a larger transducer area when compared to PZT. This optimal n is much smaller for PZT; resulting in a smaller device footprint with lower losses when considering the two devices operating at similar frequencies with similar Q's. This is due to the larger electromechanical coupling factors of PZT, a motivation for this work. Although the main challenge with PZT is increasing the Q, PZT on silicon devices provide a means for trading effective electromechanical coupling factor, k_{eff}^2, with Q.

PIEZOELECTRIC TRANSFORMER DESIGN

In addition to the use of PZT resonators for low insertion loss filters, their utility as piezoelectric voltage / current / impedance transformers may also be realized. Higher order modes and the asymmetry between the input and output electrodes, realized in the current work, is also motivated by piezoelectric transformer applications. To implement either a voltage buck or voltage boost piezoelectric transformer an approximate analysis can be followed. Assuming a low loss two port piezoelectric resonant transformer, the input power, P_{in}, is approximately equal to the output power. Based on this approximation,

$$I_{in}V_{in} \cong I_{out}V_{out} \quad (1)$$

$$V_{out}/V_{in} \cong I_{in}/I_{out} \cong \left(A_{in}N_{in}\right)/\left(A_{out}N_{out}\right) \quad (2)$$

where V_{in} is the input voltage amplitude, V_{out} is the output amplitude, I_{in} is the input current, I_{out} the output current, A_{in} and A_{out} the area of the input and output electrodes, respectively, and N_{in} and N_{out} are the number of input and output electrodes, respectively. If one desires a voltage boost piezo-transformer, the product of input area and

input number should be greater than the product of the output area and electrode number. Therefore voltage bucking or voltage boosting occurs with asymmetric input and output electrodes.

An example piezoelectric resonant transformer is depicted in Figure 1 (b)-(c). For this case, the third harmonic, $n = 3$, of the length extensional mode is under consideration. For a voltage boost configuration, the input signal drives the port with the greatest number of electrodes and the output port is connected to a resistive load which can be varied. With $A_{in} = A_{out} = L_{elec}*w_{elec}$, $N_{in} = 2$ and $N_{out} = 3$, a 2x voltage boost is expected for this particular design based on an impedance matched load. The piezoelectric transformer has a reactive load since its output is inherently capacitive. Therefore, careful consideration must be taken to assess the transformer efficiency, voltage boost / buck, and power delivery as all of these characteristics are load dependent. A detailed theoretical analysis of these trades for extensional mode PZT resonators can be found in [9].

SCATTERING PARAMETER RESULTS

The PZT on silicon resonators were fabricated on 2, 4 and 10 µm SOI wafers via a process similar to that reported in Ref. [11]. The fundamental and higher order length extensional modes ($n = 1$, 3, 5, 9 and 13 with L_{tot} = 200, 600, 1000, 1800 and 2600µm, respectively) were fabricated on 2, 4 and 10µm of silicon. For $n = 1$, L_{elec} is 196 µm and w_{elec} is 14 µm (Figure 1(a)). For $n \geq 3$ (Figure 1(b)), the electrode lengths, L_{elec} and widths, w_{elec}, are 196 and 36 µm, respectively. For all devices, the total width, w_{tot}, is 40 µm. The platinum (Pt) thickness is 100 nm and the PZT is 0.5 µm. Figure 1(c) shows images of the example devices fabricated.

The lowest loss responses of the $n = 9$ mode resonators are considered in the following. The 50 Ω terminated transmission (S_{21}) and reflection (S_{11}) frequency responses (Figure 4) were measured with a superimposed 10 V DC-bias voltage using bias-tees. Two-port calibration based on short, open, load, and through standards (GGB CSF-5) was the only calibration performed. No additional de-embedding, as was performed in Ref. [14], was done. The responses of the $n = 9$ mode resonators (0.072 mm^2) with different silicon thicknesses are compared. The impedances associated with the two port equivalent circuit in Figure 2 was extracted from the scattering parameter measurements. The extracted impedances were mathematically converted into a one-port resonator (i.e. $Z_r(s)$ electrically in parallel with $Z_{in}(s) + Z_{out}(s)$). $Q_{UL,max}$ was then extracted via a Q-circle technique, described in Ref. [15]. The expression, $Q_{UL} = \omega * \tau_{gd} * |S_{11}| / (1-|S_{11}|^2)$, was used to evaluate the frequency dependent unloaded quality factor, where τ_{gd} is the measured group delay. The maximum unloaded quality factor values, $Q_{UL,max}$, were extracted and the device metrics including the resonant frequency, f_r, minimum S_{21} insertion loss (I.L.), maximum S_{11} return loss (R.L.), effective electromechanical coupling factor, k_{eff}^2, and the extracted $R_{m,9}$ for the two device types are listed in Table I. Insertion losses as low as 2.14 dB and $Q_{UL,max}$ as high as 2850 resulted for the 2 and 10 µm

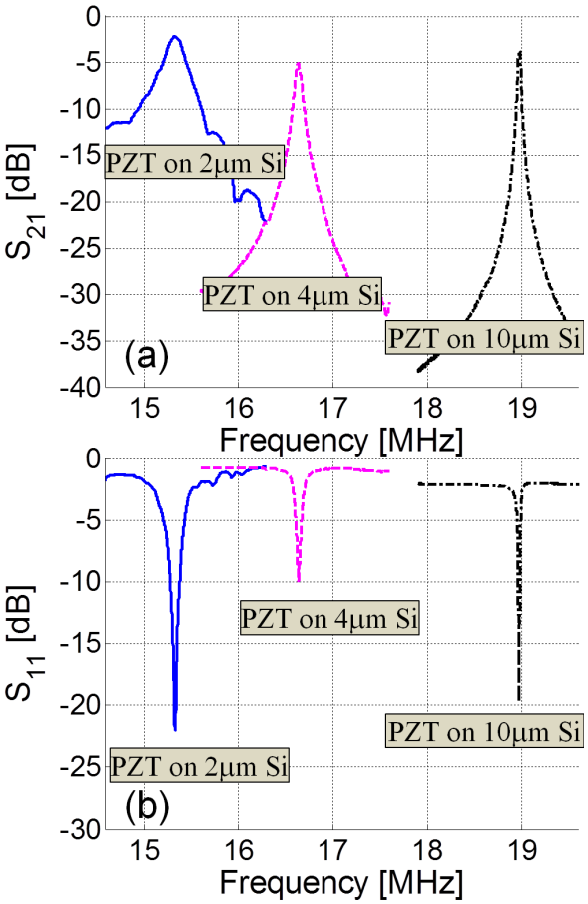

Figure 4: (a) 50 Ω terminated, forward transmission coefficient, S_{21}, of the 9th-mode resonator measured in air with 10 V DC bias on both ports. (b) Return losses, S_{11}, for the corresponding responses shown in (a).

silicon devices, respectively. A higher quality factor, with a similarly low insertion loss, results with the 10 µm silicon device due in part to the high mechanical quality factor of silicon. However, this increase in $Q_{UL,max}$ trades with lower k_{eff}^2 due to thicker device silicon. A degraded loss is due to the lower k_{eff}^2, which is extracted to be 0.38% for the PZT-on-10µm-silicon device and 3.01% for the 2 µm silicon device. This similar trend is evident when comparing the 4 µm silicon device as well. High return losses (> 20dB) also resulted for the 2 and 10 µm thick silicon devices. Motional resistances as low as 11 Ω were extracted for the PZT-on-2µm-silicon device.

Si thickness	2 µm	4 µm	10 µm
f_r [MHz]	15.329	16.634	18.967
I.L. [dB]	2.14	5.11	3.70
$R_{m,9}$ [Ω]	11	101	23
$Q_{UL,max}$	541	738	2850
R.L. [dB]	22.00	9.96	19.77
k_{eff}^2 [%]	3.01	0.85	0.38

Table 1: Summary of device performances extracted from the measurements presented in Figure 4. The maximum unloaded quality factor, $Q_{UL,max}$ is evaluated via a technique described in [15].

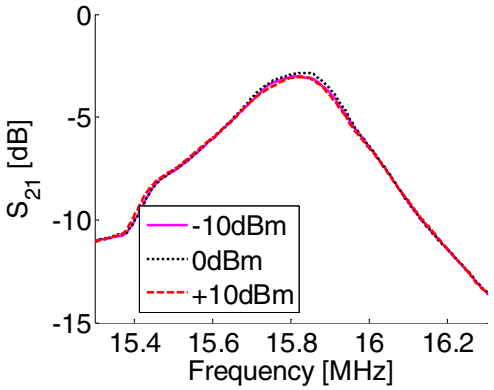

Figure 5: Frequency responses at varying input power levels (8V DC bias) for n = 9, PZT-on-2μm-Si resonator similar to that measured in Figure 4.

The device power handling characteristics were assessed by sweeping the network analyzer's source power (-10 to +10 dBm with 8 V DC bias). The frequency responses at the various power levels are shown in Figure 5 for the 9th order resonator fabricated with PZT on 2 μm silicon, a device similar to that described prior. A minimal -1% $Q_{UL,max}$ change resulted proving a significant device power handling.

The impact of increasing the transducer area was also addressed through experiments. Devices fabricated with PZT on 2, 4, and 10 μm silicon with varying n confirm these PZT device trends. The minimum insertion losses (50 Ω terminated) as function of mode number were measured and are shown in Figure 6. All measurements were taken with 10 V DC bias. The associated quality factors for the respective device are indicated in the figure. The measurements reveal an improvement in insertion loss with increased mode number, valid for $n \leq 9$ for all device thicknesses. For the 10 μm silicon devices, the improvement in $R_{m,n}$ when comparing the $n = 9$ ($R_{m,9} = 23\ \Omega$) and $n = 13$ ($R_{m,13} = 13\ \Omega$) is countered by the increase in the device capacitances; therefore, only a slight improvement in insertion loss resulted (3.70 dB versus 3.65 dB). For the 4 μm silicon devices, a degradation in the insertion loss results with larger transduction area for $n > 9$. This is attributed to both the slight increase in $R_{m,n}$ ($R_{m,9} = 30\ \Omega$ versus $R_{m,13} = 34\ \Omega$), due to a reduced quality factor, and the increased device capacitances. Similarly, the 2 μm devices did not exhibit improved insertion losses when considering the $n = 9$ and $n = 13$ modes due to both the reduced quality factor and increased capacitances.

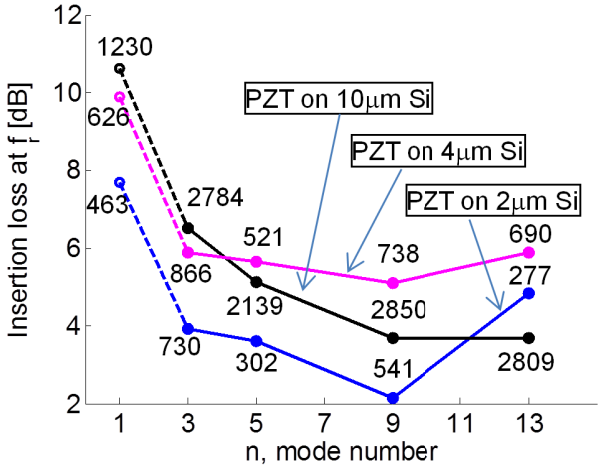

Figure 6: The measured minimum S_{21} as a function of mode number, n, for the PZT on 2, 4 and 10 μm silicon devices. These results correspond to a 10V DC bias. The devices' corresponding unloaded quality factors, $Q_{UL,max}$, are indicated.

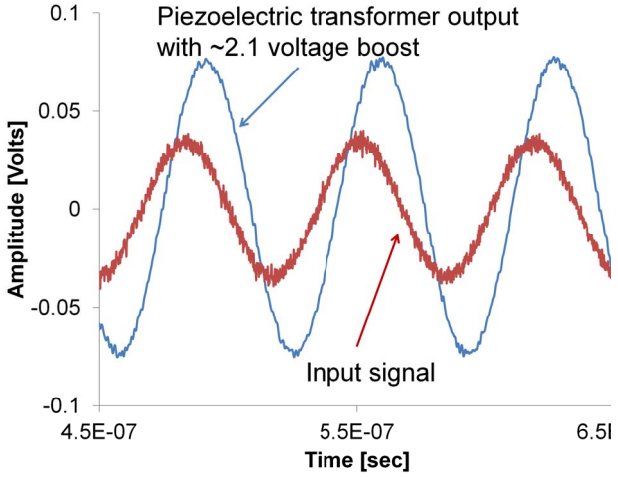

Figure 7: The measured piezoelectric resonant transformer voltage gain for the n = 3, 14.7 MHz extensional mode resonator. The resistive load is 1 MΩ.

It is clear that there is an optimal device area when considering the devices' insertion losses. For the current devices fabricated and their associated quality factors, the $n = 9$ mode resonators resulted with the minimum in insertion loss for the PZT on 2 and 4 μm device silicon. Similarly when comparing the PZT on 10 μm silicon devices, the lowest insertion loss performance resulted with the $n = 13$ mode resonator. This qualitatively agrees with the analysis and the trends shown in Figure 3.

PIEZOELECTRIC TRANSFORMER MEASUREMENTS

The PZT on 2 μm silicon resonator's transformer characteristics were evaluated. For the $n = 3$ device fabricated and shown in Figure 1 (c), a 14.7 MHz signal with a 70 mV peak to peak voltage was used to drive the piezoelectric resonator at the input port illustrated in Figure 1 (b) at its resonant frequency. The AC:AC voltage transformation characteristics were assessed by connecting the output port to a high resistive load of 1 MΩ. Both the input and output ports were DC biased at 9 V using bias T's. Figure 7 reveals the AC:AC performance of this particular device. A 150 mV peak to peak signal resulted at the output port of the resonator. This corresponds to a ~2.1 voltage gain of this particular device, thus, demonstrating its piezoelectric transformer capabilities. This compares well with the as predicted 2x voltage boost for the $n = 3$ mode resonator in the prior piezoelectric transformer analysis but it is important to note that the resistive load value directly impacts the voltage gain and efficiency.

CONCLUSIONS

This article shows PZT-on-silicon resonators exhibiting low, 50 Ω terminated insertion losses, high return losses, low motional resistances and large power handling. High performance PZT resonators fabricated on 2, 4 and 10 μm of silicon were compared. Specifically, insertion losses as low as 2.14 dB were demonstrated with a high return loss of 22 dB for the $n = 9$ resonator with 2 μm device silicon. For this mode the trade between k_{eff}^2 and quality factor with thicker device silicon were measured. The insertion losses for the fundamental and higher order extensional modes were also compared and show the trade between lower motional resistances and the increased capacitances associated with the larger transduction areas. Future work involves optimizing the device performance with respect to Q and insertion loss while demonstrating high performances at high frequencies.

In addition, the piezoelectric transformer properties were initially characterized yielding a 2.1 voltage boost under a 1 MΩ load. Future work will address the piezoelectric transformer characteristics under a variety of resistive loads. The load dependence of the transformer efficiency, power delivery and voltage gain will also be characterized.

ACKNOWLEDGEMENTS

We thank Brian Power, Joel Martin, and Luz Sanchez (US Army Research Laboratory) for the device fabrication.

REFERENCES

[1] J. Wang, Z. Ren, and C. T.-C. Nguyen, "1.156-GHz self-aligned vibrating micromechanical disk resonator," *IEEE Trans. Ultrason. Ferroelectr. Freq. Control*, vol. 51, pp. 1607-1628, Dec. 2004.

[2] H. Fatemi, R. Abdolvand, Z. Hongjun, and J. Carlisle, "Very low-loss high frequency lateral-mode resonators on polished ultrananocrystalline diamond," in *Proc. IEEE Freq. Contr.*, San Fran., CA, 2011, pp. 1-5.

[3] G. Piazza, P. L. Stephanou and A. P. Pisano, "Piezoelectric aluminum nitride vibrating countour-mode MEMS resonators" *J. Microelectromech. Syst.*, vol. 16, pp. 1406-1418, Dec. 2007.

[4] G. K. Ho, R. Abdolvand, A. Sivapurapu, S. Humad, and F. Ayazi, "Piezoelectric-on-silicon lateral bulk acoustic wave micromechanical resonators," in *J. Microelectromech. Syst.*, vol. 17, pp. 512-520, April 2008.

[5] R. H. Olsson, J. G. Fleming, K. E. Wojciechowski, M. S. Baker, and M. R. Tuck, "Post-CMOS compatible aluminum nitride MEMS filters and resonant sensors," in *Proc. IEEE Freq. Control Symp.*, Geneva, Switzerland, 2007, pp. 412–419.

[6] J. S. Pulskamp, S. S. Bedair, R. G. Polcawich, D. Judy, and S. Bhave, "Ferroelectric PZT RF MEMS resonators", in *Proc. IEEE Freq. Control Symp.*, San Francisco, CA, 2011, pp. 1-6.

[7] S. S. Bedair, D. Judy, J. Pulskamp, R. G. Polcawich, A. Gillon, E. Hwang, S. Bhave, "High rejection, tunable parallel resonance in micromachined lead zirconate titanate on silicon resonators", *Appl. Phys. Lett.,* vol. 99, pp. 103509-1-3, Sept. 2011.

[8] R. H. Olsson, K. E. Wojciechowski, M. R. Tuck and J. E. Stevens, "Microresonant impedance transformer," in *IEEE International Ultrasonics Symposium Proc.*, Rome, Italy, 2009, pp. 2153-2157.

[9] S. S. Bedair, J. Pulskamp, B. Morgan, and R. Polcawich, "Performance model of electrode tailored thin film piezoelectric transformers for high frequency switched mode power supplies," in *Proc. PowerMEMS*, Washington, DC, 2009, pp. 436–438.

[10] D. Vasic, E. Sarraute, F. Costa, P. Sangouard, and E. Cattan, "Piezoelectric micro-transformer based on SOI structure", *Sensors & Actuators A*, vol. 117, pp. 317-324, 2005.

[11] J. S. Pulskamp, S. S. Bedair, R. G. Polcawich, G. L. Smith, J. Martin, B. Power, S. A. Bhave, "Piezoelectric electrode-shaping for the excitation and detection of arbitrary modes in arbitrary geometries," *IEEE Trans. Ultrason. Ferroelectr. Freq. Control*, submitted for publication.

[12] David M. Pozar, *Microwave Engineering: 3rd Edition,* John Wiley & Sons, 2005.

[13] R. G. Polcawich and J. S. Pulskamp. "Additive Processes for Piezoelectric Materials: Piezoelectric MEMS," in *MEMS Materials and Processes Handbook*, 1st ed., R. Ghodssi and P. Lin, Ed. New York: Springer, 2011, pp. 273-344.

[14] H. Chandrahalim, S. A. Bhave, R. Polcawich, J. Pulskamp, D. Judy, R. Kaul, and M. Dubey, "Influence of silicon on quality factor, motional impedance and tuning range of PZT-transduced resonators," in *Solid State Sens., Act. & Microsyst. Work.*, Hilton Head, SC, 2008, pp. 360–363.

[15] R. Ruby, R. Parker, and D. Field, "Method of extracting unloaded Q applied across different resonator technologies," in *Proc. IEEE Ultrason. Symp.*, Beijing, China, 2008, pp. 1815-1818.

CONTACT

*Sarah S. Bedair, tel: +1-301-394-0021;
sarah.s.bedair.civ@mail.mil